EVALUATION OF FAILED HOT GAS ISOSTATIC PRESSED FUEL RODS

By
C. J. Baroch
C. B. Boyer

March 20, 1963

Vallecitos Atomic Laboratory
General Electric Company
San Jose, California

UNITED STATES ATOMIC ENERGY COMMISSION • DIVISION OF TECHNICAL INFORMATION

LEGAL NOTICE

Printed in USA. Price $1.00. Available from the Office of Technical Services, Department of Commerce, Washington 25, D. C.

USAEC Division of Technical Information Extension, Oak Ridge, Tennessee

GEAP-4206

METALS, CERAMICS, AND MATERIALS

EVALUATION OF FAILED HOT GAS ISOSTATIC PRESSED FUEL RODS

by

C. J. Baroch
Atomic Power Equipment Department
General Electric Company

and

C. B. Boyer
S. W. Porembka
Battelle Memorial Institute
Columbus, Ohio

for the

U. S. Atomic Energy Commission
under
Contract AT(04-3)-189
Project Agreement No. 11

ATOMIC POWER EQUIPMENT DEPARTMENT

GENERAL ELECTRIC

SAN JOSE, CALIFORNIA

TABLE OF CONTENTS

LIST OF ILLUSTRATIONS

LIST OF TABLES

INTRODUCTION

During the past few years, the Battelle Memorial Institute (BMI) has developed a process for the fabrication of fuel elements by hot gas isostatic pressing (gas pressure bonding). The initial process involved the joining of component parts in an inert atmosphere at high temperatures and pressures. However, it was determined that this process was also capable of producing UO_2 fuel rods in which the UO_2 density after fabrication exceeded 95 per cent of theoretical.

Because of the potential economic advantages of the process, BMI was requested by the Atomic Energy Commission (AEC) to develop the preliminary process specifications for the fabrication of high density UO_2 fuel rods. The program to develop these specifications was suspended before completion in favor of fabricating experimental fuel rods for irradiation in the Vallecitos Boiling Water Reactor (VBWR). Therefore, BMI made several fuel rods and shipped four of them to the Atomic Power Equipment Department of the General Electric Company. These fuel rods were irradiated in the VBWR under one phase of the AEC Fuel Cycle Program conducted at APED which is to conduct engineering proof tests of fuel concepts developed by other AEC contractors.

After irradiation to about 316 MWD/T and storage for about five months in the VBWR pool, the fuel rods were examined. During examination, the fuel rods broke into several pieces. Consequently, an investigation was undertaken at BMI and G. E. to determine the cause of the failure.

This report presents in detail the results of the evaluations conducted at G. E. and BMI to determine the cause of the failure. The details of the manufacturing process, VBWR irradiation, and post-irradiation history are also included in this report.

SUMMARY

Three hot gas isostatic pressed (gas pressure bonded) UO_2 stainless steel fuel rods fabricated by BMI were irradiated in the VBWR to a burnup of about 316 MWD/T. While awaiting transfer of the rods to a new assembly, the rods were stored in the VBWR pool for over five months. During the transfer of the rods from one assembly to another, one rod broke into two pieces. During subsequent pool and Radioactive Materials Laboratory (RML) examinations, all three rods broke into a total of twenty-one pieces. The failures were transverse cracking at several locations on two fuel rods and at one location on the other rod. The failures were associated with a dark reddish brown corrosion product on the clad surface. The metallurgical examination revealed that the clad in both failure and nonfailure areas contained heavy deposits of sigma phase, ferrite, and carbides in the grain boundaries and within the grains. Failure of the clad was definitely intergranular.

An investigation at BMI of non-irradiated fuel rods fabricated at the same time as the irradiated fuel rods indicated that certain areas of the clad contained as much as 0.52 per cent carbon. Subsequent investigations led to the conclusion that the inadequate removal of the binder from the UO_2

pellets resulted in the high carbon content of the stainless steel cladding. Corrosion tests in room temperature tap water indicated that the areas of clad which contained more than 0. 3 per cent carbon exhibited a rust colored corrosion product. These areas were susceptible to intergranular corrosion and became brittle after short exposures in the tap water. Areas containing less than 0. 3 per cent carbon did not exhibit the rust colored corrosion products and were not susceptible to intergranular corrosion. Neither cladding containing less than 0. 3 per cent carbon nor cladding containing greater than 0. 3 per cent carbon exhibited a rust colored corrosion product or severe corrosion after a 500 hour corrosion test in 550 F reactor grade water.

Although the cladding may have been embrittled very slightly during irradiation, intergranular corrosion, which is believed to have occurred primarily during storage of the fuel rods in the VBWR pool, was the primary cause of the failures. The high carbon content of the cladding produced this susceptibility to intergranular corrosion.

CONCLUSIONS

The metallurgical examination of the failed fuel rods and the examination of non-irradiated fuel rods at BMI led to the following conclusions:

1. Failure of the fuel rods was caused by a very high carbon content of the cladding. The high carbon content of the cladding came from the binder in the UO_2 pellets which was not satisfactorily removed during the fabricating process.
2. The high carbon content of the cladding, plus the thermal treatments in the fabricating process resulted in the formation of ferrite, carbides, and sigma phase within the grains and at the grain boundaries. The presence of sigma phase, carbides, and ferrite in the grain boundaries led to the intergranular corrosion and cracking.
3. The elimination of the binder material from the process or the complete removal of the binder in the process to preclude the effects noted in these tests can be accomplished by modification of the fabricating process. (Since the fuel rods irradiated in the VBWR were fabricated, BMI has demonstrated that isostatic pressed fuel rods can be produced from vibratory compacted powder which eliminates the need for a binder.)
4. The clad, containing large amounts of carbon, was ductile in the as-fabricated rods. However, intergranular corrosion in the VBWR and/or in the VBWR pool caused severe embrittlement.
5. The effects of irradiation during the short exposure in the VBWR is not believed to have embrittled the clad significantly.
6. Mechanical stresses, i. e., thermal cycling, differential thermal expansion of the UO_2 and stainless steel, etc., were not believed to be the cause of the failures.

DISCUSSION

Manufacture and Pretest Evaluation

As part of the overall AEC Fuel Cycle Program, BMI studied the various aspects of the hot gas isostatic pressing process for the fabrication of ceramic, cermet, and dispersion fuels. In this investigation BMI was to prepare preliminary process specifications for the production of isostatic pressed fuel rods. The program to prepare the specification was suspended before completion in favor of producing several isostatic pressed, stainless steel clad UO_2 fuel rods for irradiation in the VBWR.

The experimental program to develop the isostatic pressing techniques and the manufacturing procedure for the fabrication of the fuel rods is discussed by Paprocki.[1] The manufacturing procedure is summarized below:

The fuel consisted of a mixture of 60 w o Spencer fused UO_2 and 40 w/o superactive (ceramic) UO_2, both 5.5 per cent enriched. The superactive oxide was blended with 2.5 w/o Cerumel C binder prior to mixing with the fused oxide. Pellets of UO_2 were made by pressing the oxide at 50 tsi. The pellets were then loaded into type 304L stainless steel tubes with pressed stainless steel powder end sections. The assemblies were outgassed for one hour at 1200 F in a vacuum to remove the binder material. The sealed assemblies were then isostatically pressed for three hours at 2100 F and 10,000 psi. The resulting rods, which were 0.404 inch in diameter, were then sized through a 0.400 inch swaging die. Because of the possibility of fragmenting the UO_2 in the sizing operation, the assemblies were repressed for two hours at 2100 F and 10,000 psi.

The required fission gas plenums, center connectors, and end plugs were attached by welding to produce the full length rods.

Dimensional data for the four rods irradiated in the VBWR are listed in Figure 1. Although there are slight variations in the fuel segment lengths, the total rod lengths were maintained constant by appropriate changes in the length of center connector and the end plugs.

Destructive examination at BMI of other fuel rods fabricated at the same time as the fuel rods for irradiation, indicated that the UO_2 had a final density of 10.55 g/cc (96.3 per cent of TD) and an average O/U ratio of 2.002. The grain size of the cladding was quite large, often being more than one-half of the clad thickness (0.017 inch) in diameter. The slow cooling during the isostatic pressing cycle which produces this large grain size, also would result in the precipitation of carbides at the grain boundaries (sensitization). Consequently, 304 L (< 0.03 per cent carbon) stainless steel was used in these rods to reduce the amount of carbide precipitation.

---

(1) Paprocki, S.J., "Progress on the Use of Gas-Pressure Bonding for Fabricating Low Cost Ceramic, Cermet, and Dispersion Fuels," BMI-1555, November, 1961.

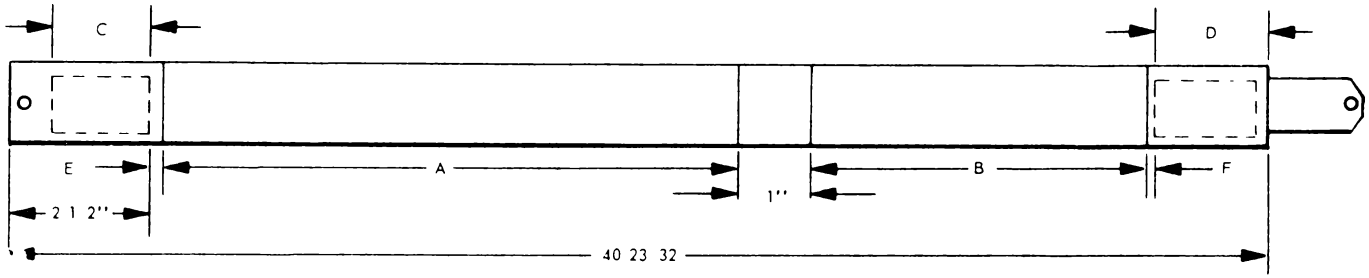

ROD	AVG DIAM OVER A	AVG DIAM OVER B	CORE LENGTH A, IN.	CORE LENGTH B, IN.	TOTAL LENGTH OF CORE IN	TOTAL CORE WT g	PLENUM LENGTH C IN.	PLENUM LENGTH D IN.	SPACER THICKNESS E	SPACER THICKNESS F
1	0.3965	0.3965	24 3 8	11 11 16	36 1 16	636	1 3 16	41 64	1 16	1 16
2	0.397	0.397	24 5 16	11 1 2	36 13 16	634	1 13 64	31 64	3 64	3 64
3	0.3975	0.397	24 7 32	12 1 16	36 9 32	640	1 3 16	33 64	1 16	1 16
4	0.3975	0.397	24 5 32	12 1 8	36 9 32	642	1 3 16	33 64	1 16	3 64

AVERAGE CLADDING THICKNESS 17 MILS

AVERAGE PLENUM WALL THICKNESS 37 MILS

PLENUM SPACERS CONTAIN A 62 MIL DIAMETER HOLE

1136–1

Figure 1. Final Dimensions of Four Isostatic Pressed UO_2 Fuel Rods Fabricated for VBWR Irradiation Program

Steam corrosion tests, 48 hours in 750 F steam, of samples of isostatic pressed clad showed no abnormal surface effects or excessive weight gains. One comparison rod was thermal cycled for 50 times between room temperature and 1000 F without showing any growth or change in surface conditions.

Four isostatic pressed fuel rods were received at APED on September 9, 1961, and underwent further nondestructive examination. This examination indicated that the surface of the rods was quite rough with frequent indentations, particularly at pellet interfaces as shown in Figure 2. Diameter measurements which were made along the lengths of the rods showed that the deepest depression was about 0.033 inch. All four rods had at least a 0.040 inch bow over a length of 40-3/4 inches: the maximum bow was 0.060 inch.

Three of the fuel rods were put into a Fuel Cycle Special Assembly, designated 4L. The fourth rod was held out for intentional defecting and was scheduled for testing at a later date. The 4L assembly also contained a large centermelt calibration rod and four corner tie rods. Various views of the assembly are shown in Figures 3, 4, 5 and 6. The isostatic pressed rods can be identified by their rough surfaces. The lower end plug shafts of the fuel rods are set into holes in the lower tie plate. The rods are held down by blades and pins attached to the handle. In this assembly, the BMI rods were free to expand approximately 1/4 inch more in length than the corner tie rods.

Irradiation in the VBWR

Reactor Operation: The 4L assembly was inserted into position 0-9 (average heat flux for the BMI rods at 30 MW power of 117,000 Btu/hr-ft^2, peak of 175,000) in the VBWR on December 21, 1961. To satisfy VBWR operating license requirements an assembly containing a new fuel concept must first be operated at a peak flux of less than 250,000 Btu/hr-ft^2 and visually inspected before operating at a higher heat flux. The 4L assembly operated satisfactorily throughout run 137. After run 137 the 4L assembly was visually inspected and no defects were noted. The assembly was transferred to position J-12 (average heat flux for the BMI rods at 30 MW power of 298,000 Btu/hr-ft^2, peak 449,000) for run 138.

The 4L assembly was in the VBWR for almost 25 days. During that time the reactor was critical for 486 hours and was at temperature (546 F) for 439 hours. The integrated fast flux (>1 mev) at the peak location of the BMI rods was about 3×10^{19} nvt.

During runs 137 and 138 there were 15 reactor scrams. The duration of the shutdowns as indicated in Table I ranged from 14 to 813 minutes. The scram of 813 minutes duration was for reactor shutdown at the completion of run 137 and before startup of run 138. A plot of reactor power versus time is shown in Figure 7. The heat flux at any given time experienced by the rods can be obtained by multiplying the heat flux at 30 MW by the ratio of the reactor power at any given

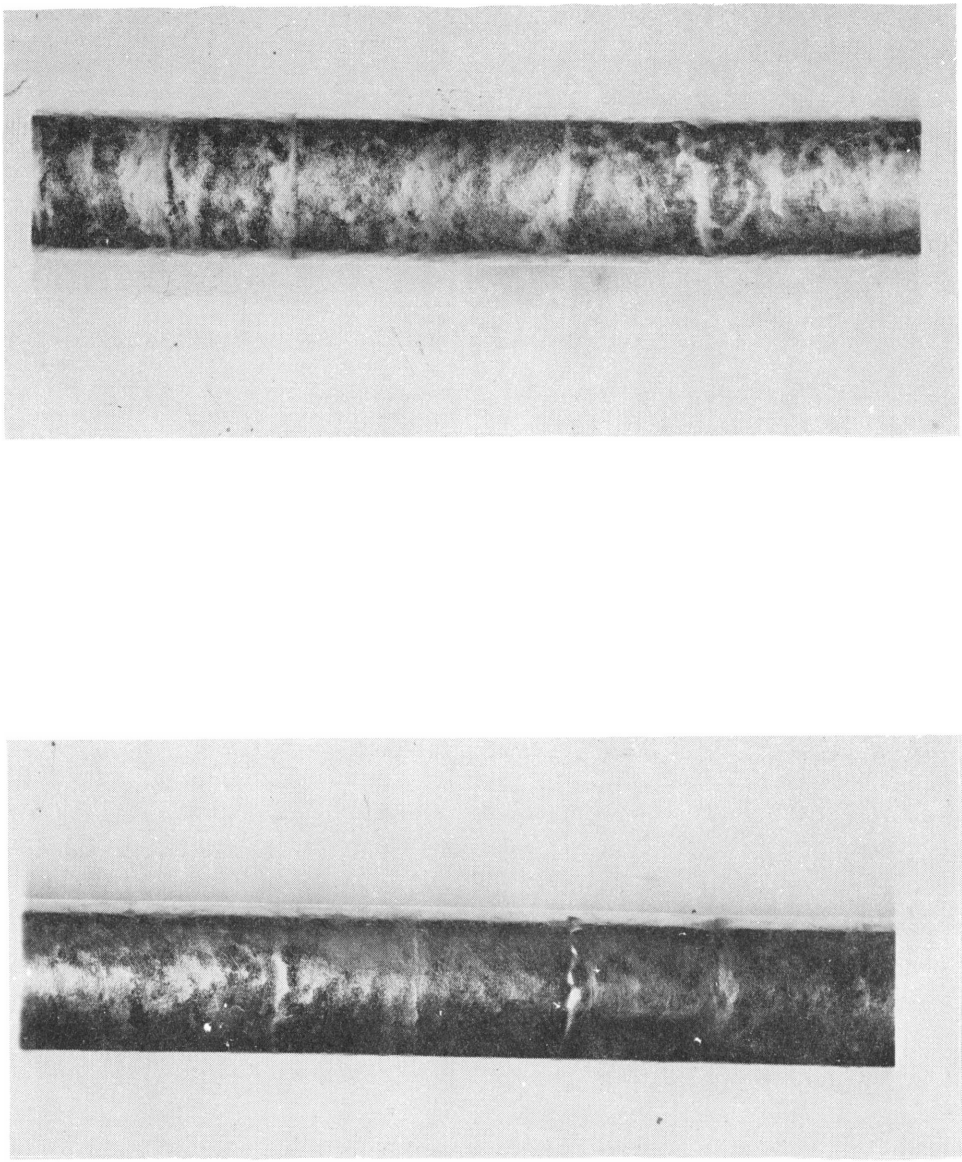

1136–2

FIGURE 2 TYPICAL SURFACE OF ISOSTATIC PRESSED FUEL RODS

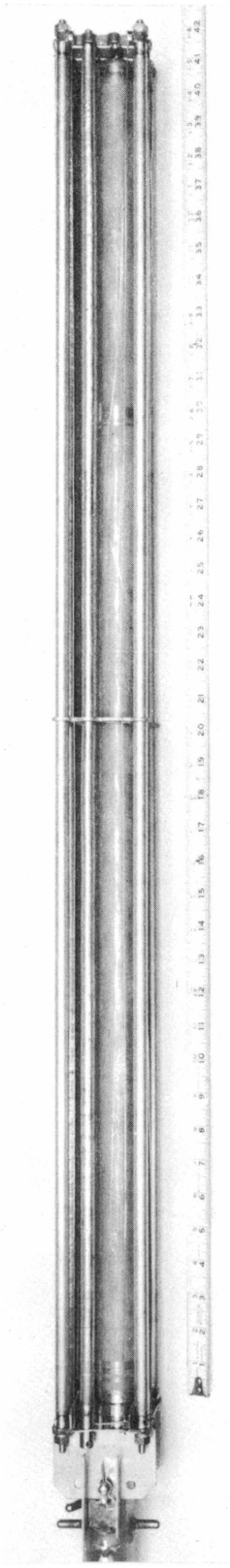

522-13

FIGURE 3 SIDE VIEW OF ASSEMBLY 4–L

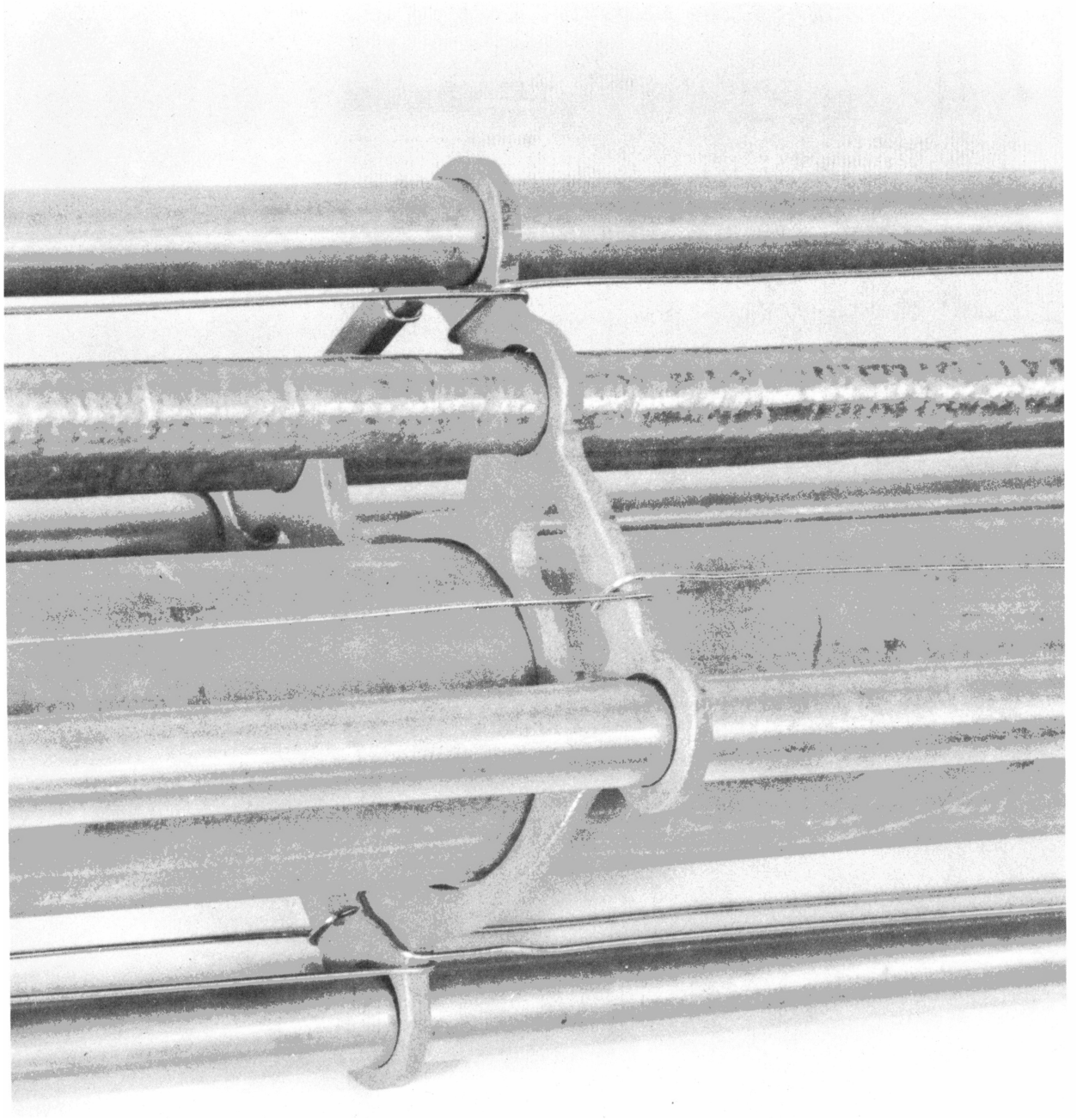

522-14

FIGURE 4 ISOTATIC PRESSED AND CENTER MELT CALIBRATION ROD ARRANGEMENT IN ASSEMBLY 4–L

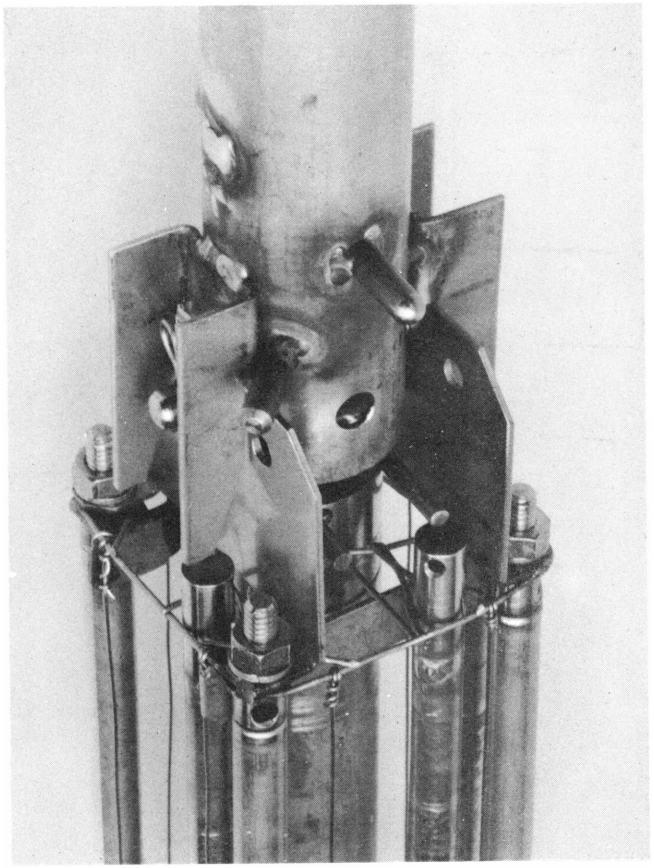

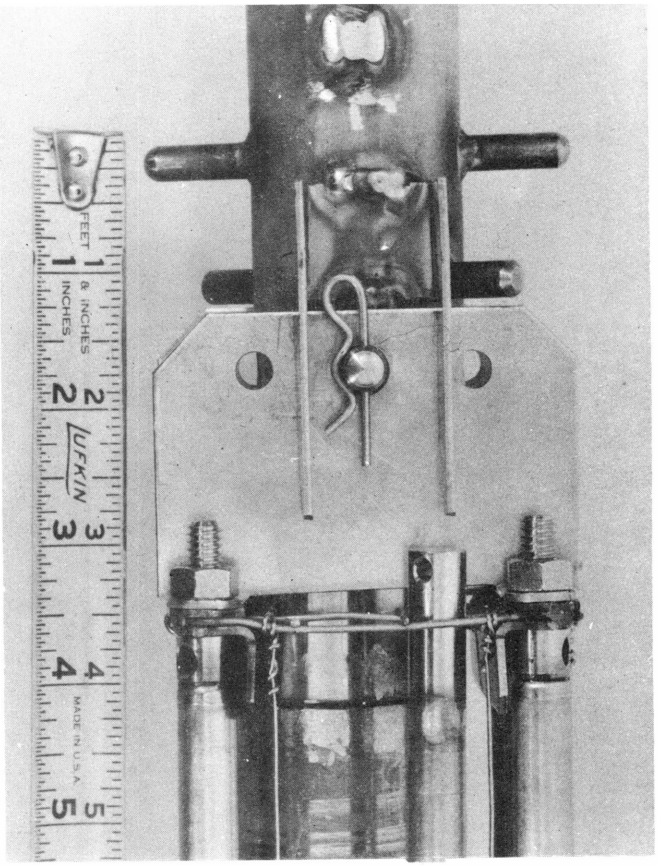

522-15

FIGURE 5 QUICK DISCONNECT FOR ASSEMBLY 4-L, SHOWING RETAINER CLIP (RIGHT PHOTO) AND ROD HOLD-DOWN ARRANGEMENT (LEFT PHOTO)

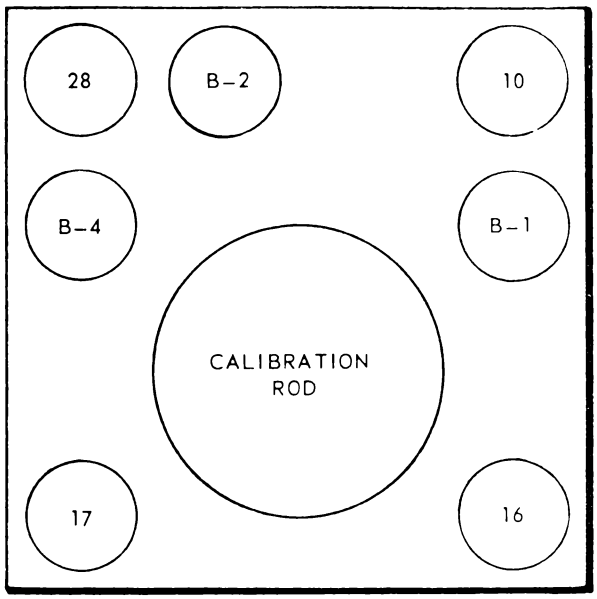

DESCRIPTION OF FUEL RODS IN 4-L ASSEMBLY

CODE NO.	ROD DESCRIPTION	DIAMETER OF ROD IN.	FUEL LENGTH IN.	WT OF FUEL gms	FUEL ENRICHMENT %
10	TIE ROD	0.400	36 15. 16	660	3.9
16	TIE ROD	0.400	37 1/8	679	3.9
17	TIE ROD	0.400	37 1. 16	675	3.9
28	TIE ROD	0.400	37 1 8	675	3.9
B-1	BMI ROD	0.397	36 1. 16	636	5.58
B-2	BMI ROD	0.397	36 13 16	634	5.58
B-4	BMI ROD	0.398	36 9. 32	642	5.58
	CALIBRATION ROD	1.38		7230	3.9

1136-3

Figure 6. Top View of Loading Diagram of 4-L Assembly

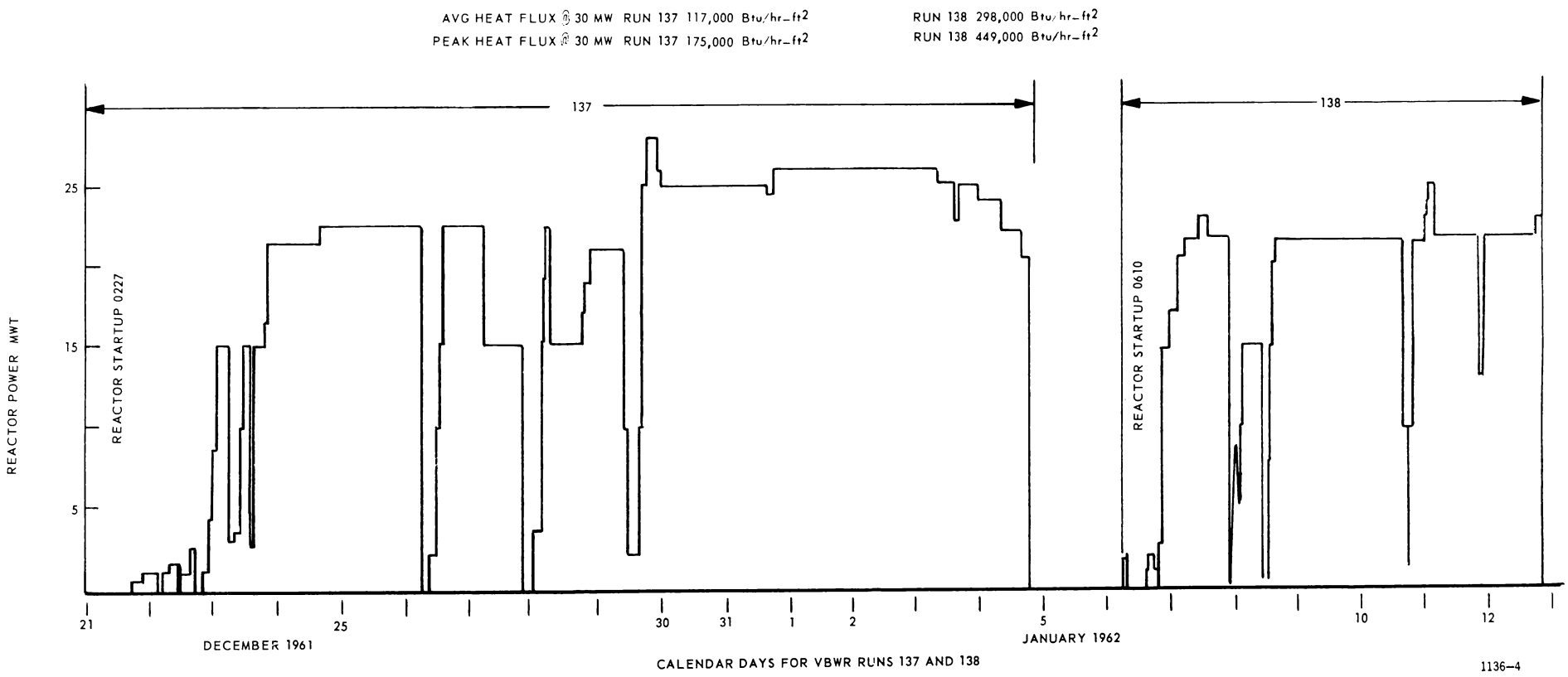

FIGURE 7 PLOT OF REACTOR POWER VERSUS TIME FOR RUNS 137 AND 138

Figure 7. Plot of Reactor Power Versus Time for Runs 137 and 138

time to 30 MW. Although the reactor requires several hours to cool down to room temperature, there was undoubtedly severe strain and thermal cycling of the fuel rods during the scrams. There also was some thermal cycling when the power level of the reactor was changed by more than about 10 MW.

TABLE I

RESUME OF REACTOR SCRAMS FOR VBWR RUNS 137 AND 138

Number	VBWR Run	Date	Time	Duration (minutes)	Remarks
1	137	12/22/61	0325	55	
2	137	12/22/61	0510	124	
3	137	12/22/61	1025	125	
4	137	12/22/61	1523	52	
5	137	12/22/61	1730	167	
6	137	12/26/61	0708	93	
7	137	12/27/61	2015	73	
8	137	1/4/62	1917	18	
9	137	1/4/62	2049	813	Reactor Shutdown
10	138	1/6/62	0730	268	Reactor Shutdown
11	138	1/6/62	1220	86	
12	138	1/6/62	1406	26	
13	138	1/6/62	1819	14	
14	138	1/7/62	2155	26	
15	138	1/12/62	2055		Reactor Shutdown

Water Chemistry: Throughout the power runs, the water in the VBWR is monitored. Samples of the water are analyzed daily or more frequently when the analyses indicate a buildup on the impurity levels has occurred. The analyses include the measurement of the amount of crud, resistivity and chloride ion content. The reactor water is not analyzed for oxygen, however, it has been calculated that the average oxygen content of the water caused by radiolytic action is 0.2 to 0.3 ppm and that of the steam is 20 to 30 ppm. There is no pH control of the water other than that produced during the deionization. The reactor water at room temperature generally has a pH of about 7.

The analysis for the chloride ion content and conductivity of the reactor water during runs 137 and 138 are listed in Table II. The chloride ion content of the water exceeded 0.1 ppm on two occasions and reached a maximum level of 0.6 ppm on December 30, 1961.

Fission Gas Release: The amount of activity caused by the release of fission product gases is monitored continuously during the operation of the VBWR. In the VBWR, which is primarily a test reactor, there is occasionally a moderate level of fission gas activity measured at the exhaust stack during the testing of intentionally defected fuel elements. During runs 137 and 138

however, there was about 250μ curies per second of unexplained activity from the fission gases. The analysis of the fission gas activity data did not reveal whether this activity could be attributed to a failure of the BMI rods or some other elements.

TABLE II

CHEMICAL ANALYSIS OF THE REACTOR WATER DURING RUNS 137 AND 138

Run 137

Date	Time	Cl, ppm	Power MWt	Remarks*
12/21/61	0900	< 0.020	0	
12/22/61	0610	< 0.020	1	Conductivity 1.0μ mho at 25°C
12/23/61	--	--	--	
12/24/61	0215	0.026	21.5	
12/25/61	0620	0.050	22.5	
12/26/61	0624	0.040	22.5	
12/27/61	0405	0.034	22.5	
	1825	< 0.020	15	
12/28/61	0635	0.020	22.5	
12/29/61	0610	0.050	21	
	1950	0.125	32	
12/30/61	1310	0.60	25	
	1745	0.35	25	
	1900		25	Conductivity 2.67μ mho at 25°C
	2240	0.185	25	Conductivity 1.65μ mho at 25°C
12/31/61	0140	0.027	25	Conductivity 1.16μ mho at 25°C
	0600	0.014	25	Conductivity 0.83μ mho at 25°C
	1900	< 0.020	26.6	Conductivity 0.55μ mho at 25°C
1/1/62	1830	< 0.020	26	Conductivity 0.55μ mho at 25°C
1/2/62	0928	--	26	
1/3/62	0515	< 0.020	25	
1/4/62	0515	< 0.020	24	
			Run 138	
1/6/62	--	--	--	Run 138 begins
1/7/62	0220	< 0.020	18	
1/8/62	0615	< 0.020	15	
1/9/62	0400	< 0.020	21.5	
1/10/62	0917	< 0.020	21.5	
1/11/62	0330	0.030	21.7	
1/12/62	0500	0.056	21.7	
	0937	0.095	21.7	
	1345	0.012	21.7	

*pH of the water is maintained at about 7 by maintaining resistivity at 1 megohm. No chemical additions are made.

Post Irradiation History

After run 138 was completed, the 4L assembly was transferred from the reactor to the storage pool in order to remove a rod which was part of another experiment, a UO_2 central melting calibration rod. During the removal operation on January 16, 1962, a force large enough to break the 60 mil stainless steel spacer was required to extract the calibration rod from the assembly. The difficulty in extracting the calibration rod, however, in no way damaged it, and it is believed that the removal operation did not materially affect the integrity of the BMI rods.

Because of the damage to the 4L assembly, it was decided to manufacture a new assembly to accommodate other fuel rod concepts and a defected BMI rod as well as the BMI rods irradiated in the original 4L assembly. Consequently, the original assembly containing the BMI rods was placed in an aluminum can and stored in the VBWR pool until June 1962, when the new 4L assembly was ready for insertion of the irradiated BMI rods.

The water in the pool is ordinary tap water and only the pH level is controlled. Attempts are made to maintain the pH at 7, but it varies between 5.5 and 8. The pool water is seldom analyzed and there were no chemical analyses run from January to July. However, a sample of the water taken on July 7, 1962, had a pH of 6.2 and a conductivity of 433μ mho's and contained 7.6 ppm chloride ion and 6.1 ppm dissolved oxygen. On June 20, 1962, the new 4L assembly containing all the fuel rods, except the irradiated BMI rods, was put into the pool and prepared for insertion of the irradiated BMI rods. The first two BMI rods (BMI-1 and -2) were removed from the original 4L assembly and the corrosion film was removed by wiping with a cloth. The rods were then inserted into the new assembly. However, during the removal of BMI-4 rod an eight-inch long segment broke off from the remainder of the rod. The other 32 inches of the rod remained in the assembly, but no difficulties were encountered in extracting this portion of the rod from the assembly. The pieces of the BMI-4 rod were put in a 3/4 inch stainless steel storage tube.

An attempt was made to determine the cause of the failure of BMI-4 rod by examining it in the VBWR pool using a periscope. During the examination, the 32-inch segment was allowed to slide out of the storage tube maintained at an angle of about 30 degrees with the inspection table. When about 6 inches of the 32-inch section were visible, the six-inch section fell to the table. The remaining 26-inch section and the 8-inch section were removed from the storage tube without incident. However, during subsequent examination the 8-inch section was again slid out of the storage tube in the manner described above. When 5 inches of the 8-inch section were visible, the 5-inch section fell to the table. The remaining 3-inch section slid out of the tube without fracturing. During the examination of the BMI-4 rod, several photographs were taken and the magnetic properties of the rod were tested using a horseshoe magnet. There was not any noticeable attraction of the magnet to the rod. Consequently, it was concluded that the steel did not contain any significant amounts of ferrite. The photographs taken in the pool do not show anything which is not shown more clearly in the photographs taken during the RML examination.

After photographing the pieces of BMI-4 rod, they were returned to the storage tube. The BMI-2 rod was then removed from the new 4L assembly without incident. However, when attempting to remove the BMI-1 rod from the new 4L assembly, the top 6 inches separated from the rest of the rod. The remaining part of the BMI-1 rod was pried out of the bundle at which time it developed a double dog leg. When attempting to straighten the rod, it broke into several pieces. All segments of all three rods were then put into an RML transfer can and shipped to RML for further inspection.

Metallurgical Examination of Failed Rods

Preliminary RML Examination: The failed BMI rods received a preliminary examination prior to the detailed metallographic examination. This examination included:

1. Visual inspection of several fuel rod sections and the entire BMI-2 rod.
2. Diametral and longitudinal measurements of BMI-2 rod and diametral measurements of a segment from BMI-1 rod.
3. Selection of fuel rod sections to be examined metallographically.
4. Determination of the bending strength of a sound section of the BMI-4 rod.

Several segments of the fuel rods and the BMI-2 rod were visually examined to determine the course of the failures. During handling, the BMI-2 rod also fractured in one location. The BMI-1 and BMI-4 rods were reassembled to determine the location of the fractures. Gamma scanning of the fuel rod segments was used to aid in the reassembly of the rods and to insure that the reassembly was correct. The location of the fractures was then determined by measurement made by gamma scan and the reassembled rod. A sketch of the three fuel rods and the approximate location of the failures are shown in Figure 8.

A tie rod of the 4L assembly was also examined to determine whether cracking occurred in a standard VBWR rod. No cracks or failures were observed nor was there any unusual appearance in the corrosion product. It was apparent that the failure of the rods was inherent in the isostatic pressing process rather than in the 4L assembly.

Visual examination of the rods revealed that all of the known failures occurred in areas which exhibited a dark reddish brown deposit of a corrosion product. However, there were areas in which the corrosion product was present and no cracking occurred. All of the failures in these rods occurred over the fueled sections, and there was no evidence of failures in the plenum, end caps, or connecting rods. However, there was no pattern associated with the failures which would indicate whether the failures could be associated with peak heat flux or spacer location. Examination of the fracture surfaces indicated the following:

1. There has been no thinning of the clad either by corrosive action or by penetration of the metal with UO_2.

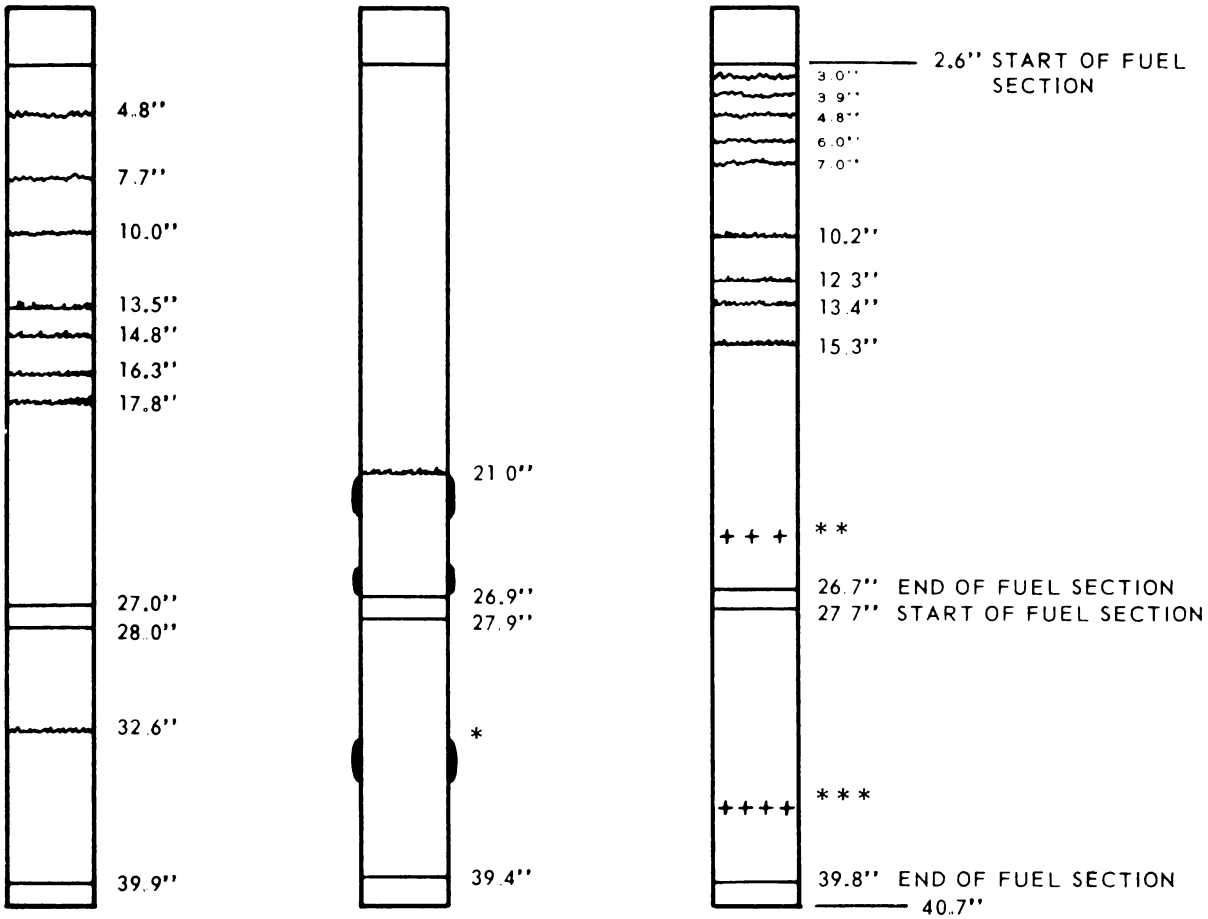

* AREA OF ABNORMAL INCREASE IN DIAMETER

** ARTIFICIAL FRACTURE IN AREA NOT EXHIBITING RED BROWN CORROSION PRODUCT

*** ARTIFICIAL FRACTURE IN AREA EXHIBITING A RED BROWN CORROSION PRODUCT

1136–17

Figure 8. Location of Fractures in the BMI Rods

2. There appears to be bonding between the clad and the UO_2 since several samples exhibited areas where the clad had been peeled back and the UO_2 particles were firmly attached to the clad.

3. There were areas in the UO_2 on which corrosion products had been deposited. Also, there was the possibility of some chemical attack of the UO_2 since at least two fracture faces exhibited a variance in the color and appearance of the UO_2 which was not typical of the UO_2 coated with a corrosive product.

4. From 10 to 90 per cent of the clad on the fracture surface was generally coated with a corrosion product. The remaining surface was bright and shiny; typical of a freshly fractured surface, and seemed to be somewhat ductile.

5. The cracking followed a very irregular pattern which is typical of an intergranular attack.

Diametral and longitudinal measurements were taken of the BMI-2 rod as well as diametral measurements of the 3-inch segment of BMI-1 rod. A plot of the diameter of the BMI-2 rod after irradiation along the length at two different radial angles is shown in Figure 9. This figure also includes the pre-irradiation measurements. At two locations there has been some increase in the diameter of the BMI-2 rod, but there was no increase in the diameter of the 3-inch segment of BMI-1 rod. Whether the increased diameter is actually caused by swelling of the rod, by surface irregularities prior to irradiation, or by deposition of a corrosion product was not determined. Measurement of the rod after cleaning with a wire brush, however, did not result in any significant change in the diameter of the rod. The longitudinal measurements which were made are of insignificant value because of the difficulty in precisely matching the fracture faces. Photographs of the failed BMI rods are shown in Figures 10 through 12. Front and rear views of the fracture in BMI-2 rod are shown in Figure 10. The appearance of three different fractures from unidentified fuel rods is shown in Figure 11. A close-up view in the area of the connector pin of BMI-4 rod is shown in Figure 12.

A 24-inch section of the BMI-4 rod which did not contain any visible fracture was subjected to a bending test to determine whether there were any other areas of weakness in the rod. The rod was supported at both ends and positioned at an angle of about 45 degrees with the horizontal. A downward force was applied at the center of the rod with the "slaves" and the rod broke with very little force being applied in an area exhibiting a reddish brown corrosion product. The test was repeated on the remaining 20-inch section and the rod broke this time in the middle in an area not exhibiting the reddish brown corrosion product. The downward force required to cause this fracture was estimated to be about 15 pounds. The location of these fractures are shown in Figure 8.

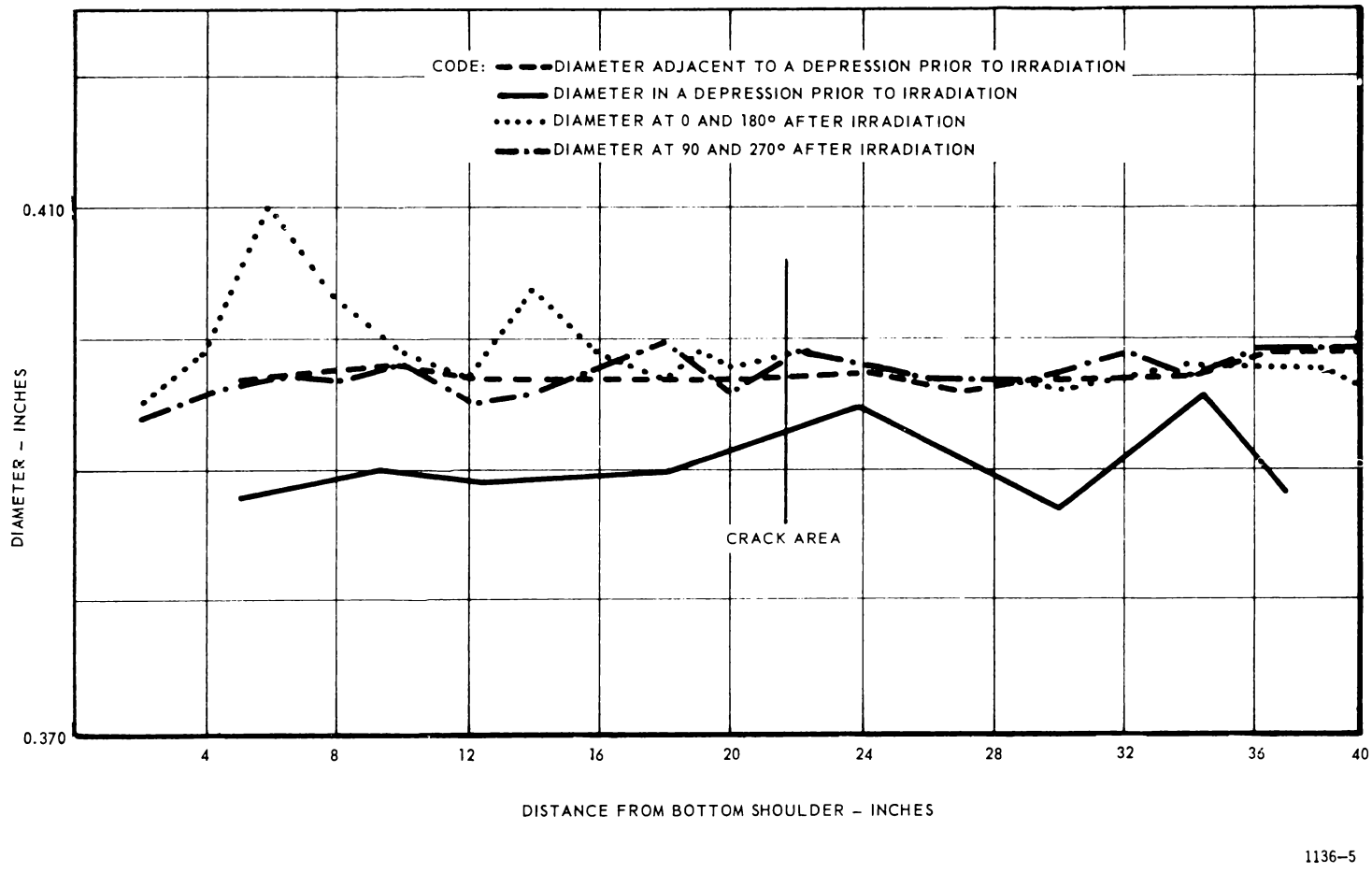

Figure 9. Pre- and Post-Irradiation Measurements of BMI-2 Rod

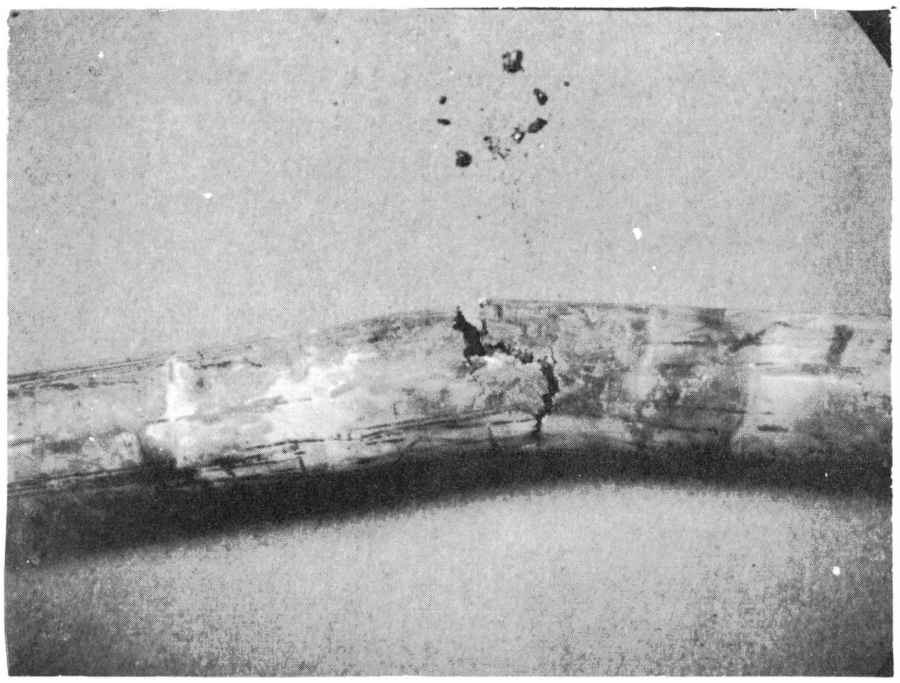

FRONT SIDE OF CRACK

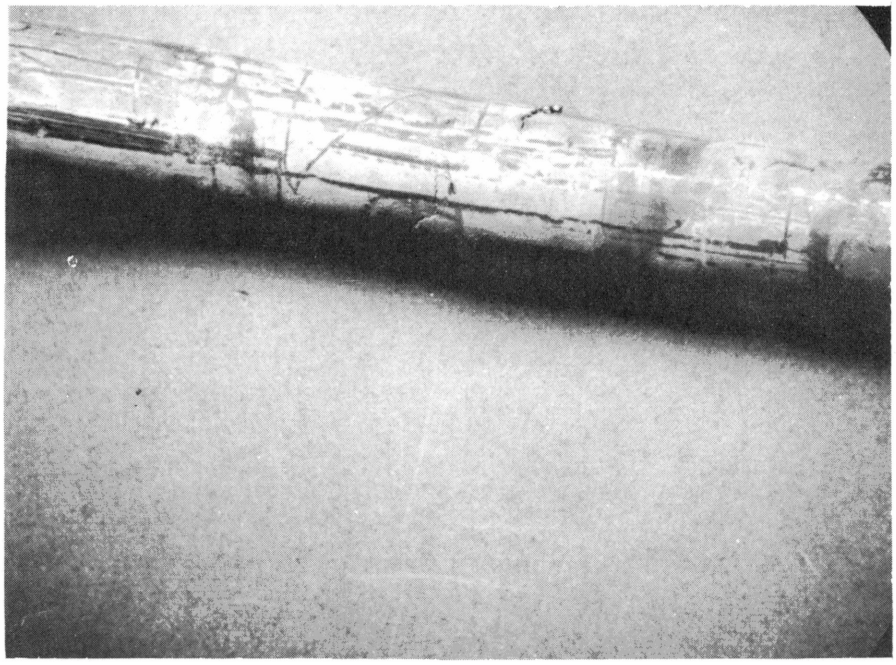

1136–6

BACK SIDE OF CRACK

FIGURE 10 LONGITUDINAL VIEW OF FAILURE IN BMI–2 ROD. NOTE THE DARK COLORED DEPOSIT SURROUNDING THE FRACTURE AREA, PARTICULARILY ON THE FRONT SIDE

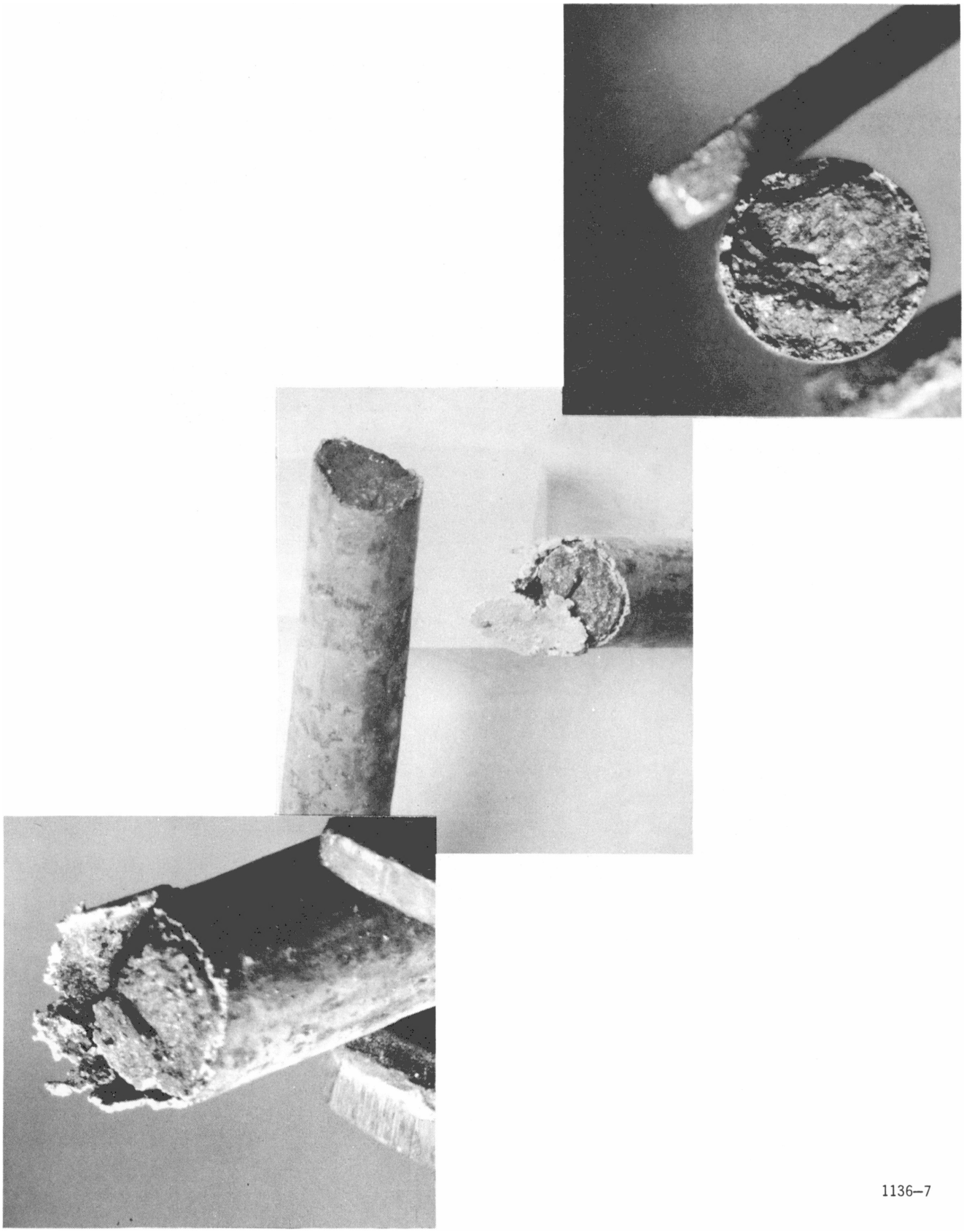

FIGURE 11 APPEARANCE OF THREE DIFFERENT FRACTURES FROM AN UNIDENTIFIED BMI ROD

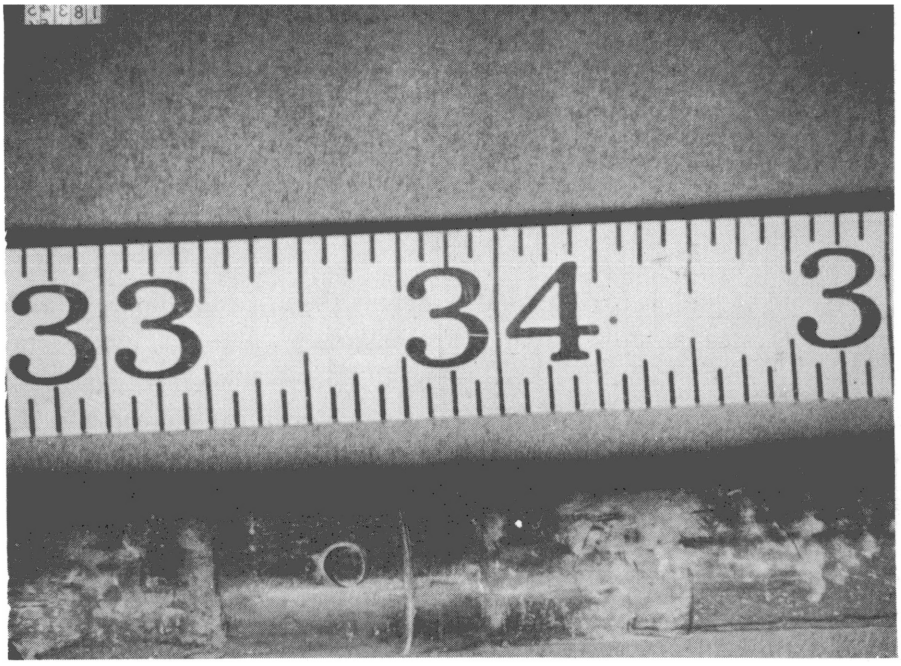

1136–8

FIGURE 12 CLOSE UP OF PIN AREA OF BMI–4 ROD. NOTE THE CLEAN APPEARANCE FOR ABOUT 1/2 INCH ON EACH SIDE OF THE PIN.

The preliminary RML examination did not reveal the cause of the failures. However, corrosion appeared to be a significant factor in causing the failures. The nature of the corrosion products indicated that corrosion had been in progress for quite some time and that removal of the rods from the 4L assembly was not the cause of the fracturing.

Metallographic Examination: Two specimens from BMI-2 rod underwent detailed metallographic examination. One specimen was a longitudinal section of the rod taken from an area which did not contain a failure and which did not exhibit a red brown corrosion product. The other specimen was a longitudinal section which contained the fracture shown in Figure 10. Originally, a third specimen from either the BMI-2 or BMI-4 rods was to be examined. However, the BMI evaluation of non-irradiated fuel rods had determined the cause of the failures before the RML examination was initiated. Therefore, it was considered unnecessary to examine more than two specimens.

Figures 13 through 18 are some of the photographs taken during the metallographic examination. A reaction zone between the UO_2 and stainless steel and permeation of the UO_2 by the stainless steel as indicated by the presence of a metallic phase in the UO_2 are shown in Figure 13. The appearance of the clad on both the inside and outside surfaces are shown in Figure 14. Large amounts of grain boundary precipitate, hair line cracking, and large grain size in the stainless steel clad from a non failure area are also shown in Figure 14.

A composite photograph of the unetched clad in the vicinity of a failure is shown in Figure 15a. This photograph indicates that there is wide variation in the metallurgical structure of the clad. For example, there are areas in which there is a large amount of grain boundary precipitate while in other areas, there is considerably less grain boundary precipitate. This figure indicates that there are many hairline cracks in the clad which did not result in fracturing of the fuel rod, but certainly reduced the integrity of the rod. A composite photograph of the same section after etching with Vilellas' reagent is shown in Figure 15b. These photographs also demonstrate the wide variation in the metallurgical structure of the clad, even in a one-inch longitudinal section. Many of the areas which did not show a grain boundary precipitate in the unetched condition do, however, contain some precipitate at the grain boundary and within the grains as shown by comparing Figure 15a with Figure 15b.

A composite photograph of the clad sample taken from a nonfailure area is shown in Figure 16a. Even in a nonfailure area, there are large amounts of precipitate in the grain boundaries, within the grains, and on twin faces. There are no hairline cracks visible in this photograph, however, the large amount of precipitate at the grain boundaries indicates that this area of the clad could be quite susceptible to intergranular corrosion and/or cracking. There is some evidence of intergranular corrosion as indicated by the heavy film surrounding some of the grains in the left side of the photograph. An enlarged photograph more clearly defining one of these grains is shown in Figure 16b.

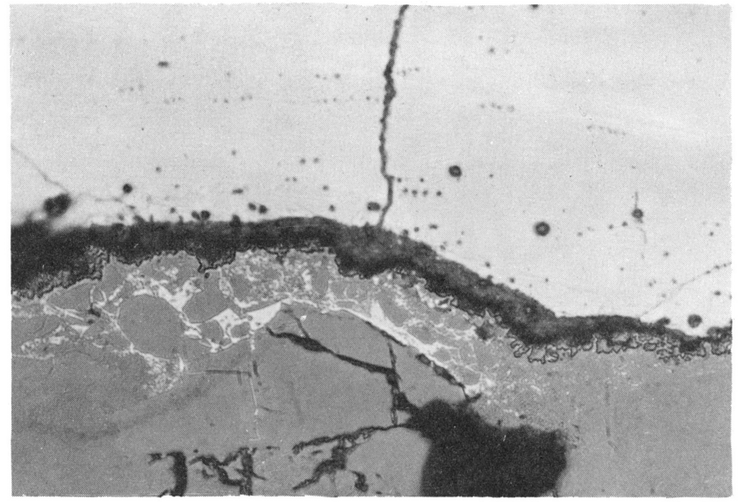

MAGNIFICATION: 500X

ETCHANT: VILELLA'S

COMMENTS: NOTE THE REACTION ZONE BETWEEN THE UO_2 AND CLAD AND THE METALLIC PHASE IN THE FUEL.

FIGURE 13 EVIDENCE OF REACTION BETWEEN UO_2 AND CLAD

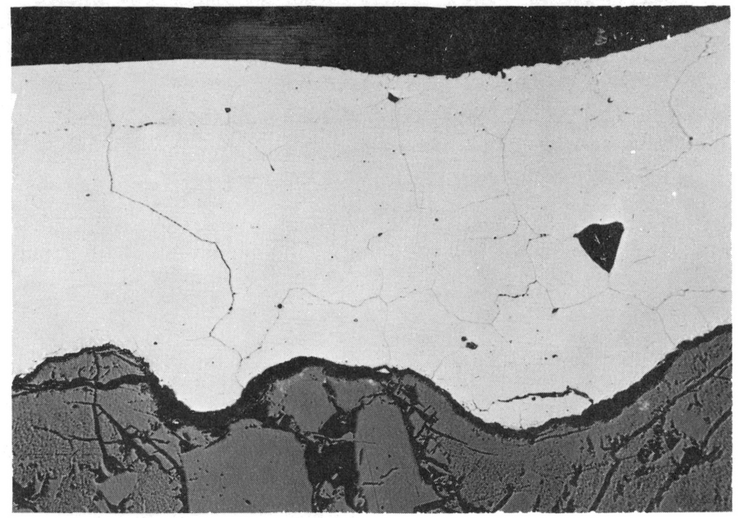

MAGNIFICATION: 100X

ETCHANT: NONE

COMMENTS: NOTE THE HEAVY GRAIN BOUNDARY PRECIPITATE, HAIR LINE CRACKS, DISTORTED CLADDING, AND PENETRATION OF CLAD INTO UO_2.

1136-9

FIGURE 14 APPEARANCE OF AS-POLISHED CLAD IN NON-FAILURE REGION

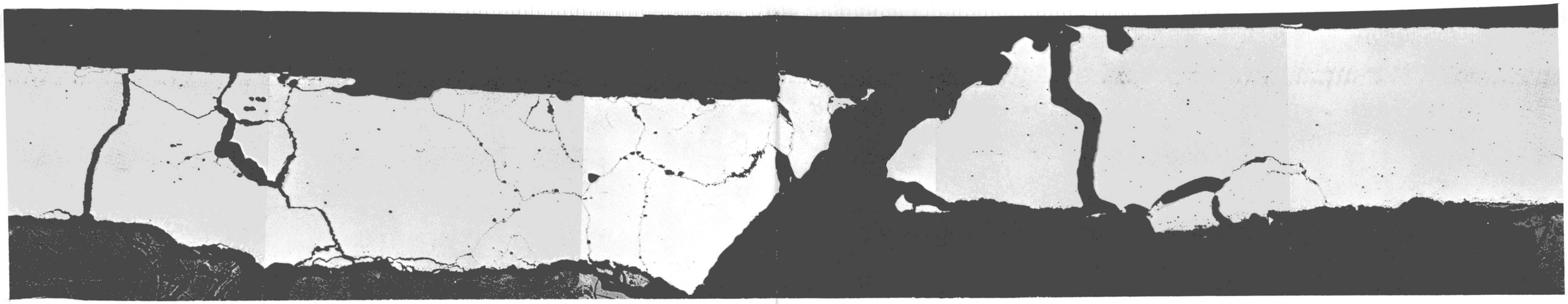

(a)

AS POLISHED

(B)

ETCHED WITH
VILELLA'S REGENT

1136–10

FIGURE 15 APPEARANCE OF CLAD IN A LONGITUDINAL SECTION OF THE FUEL ROD IN THE AREA OF FAILURE

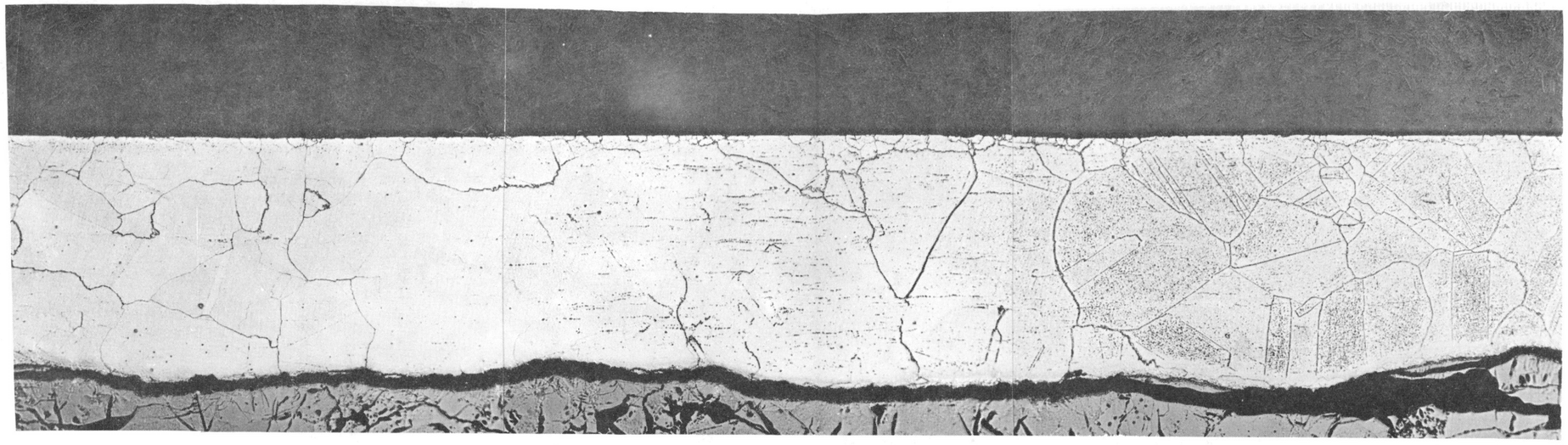

(A) MAGNIFICATION: 100X
ETCHANT: VILELLA'S REAGENT

(B) MAGNIFICATION: 500X
ETCHANT: VILELLA'S REAGENT

1136–11

Figure 16. Appearance of Clad in a Non-Failure Area - Hot Gas Isostatic Pressed Rods, Assembly 4-L

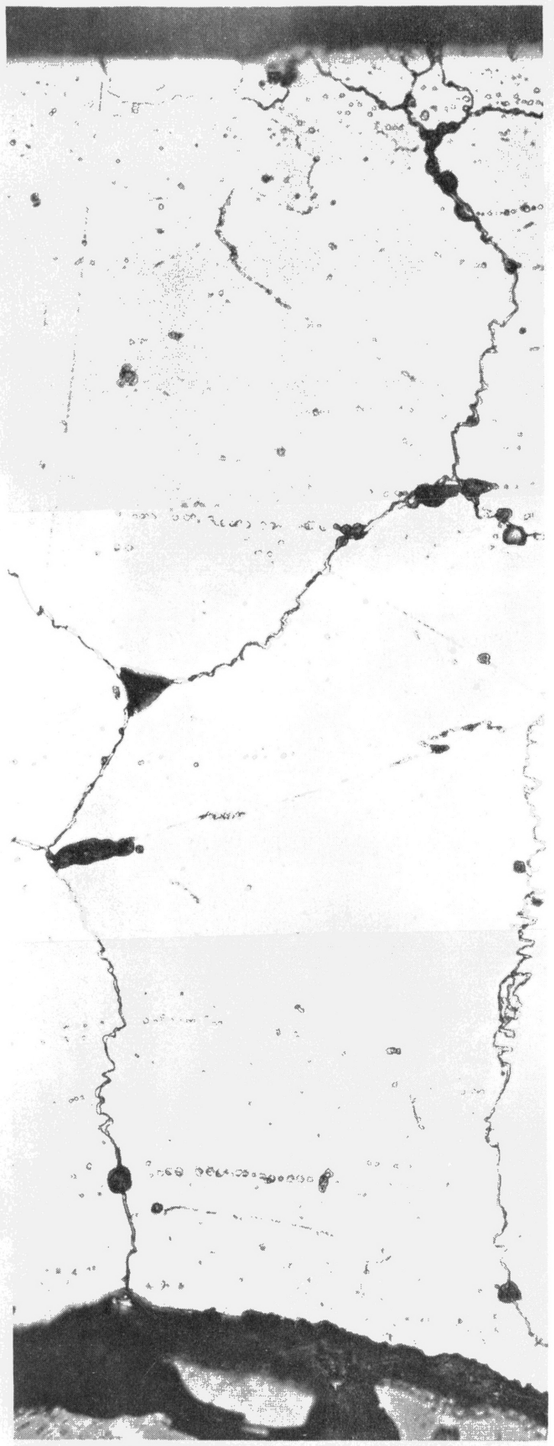

(B)

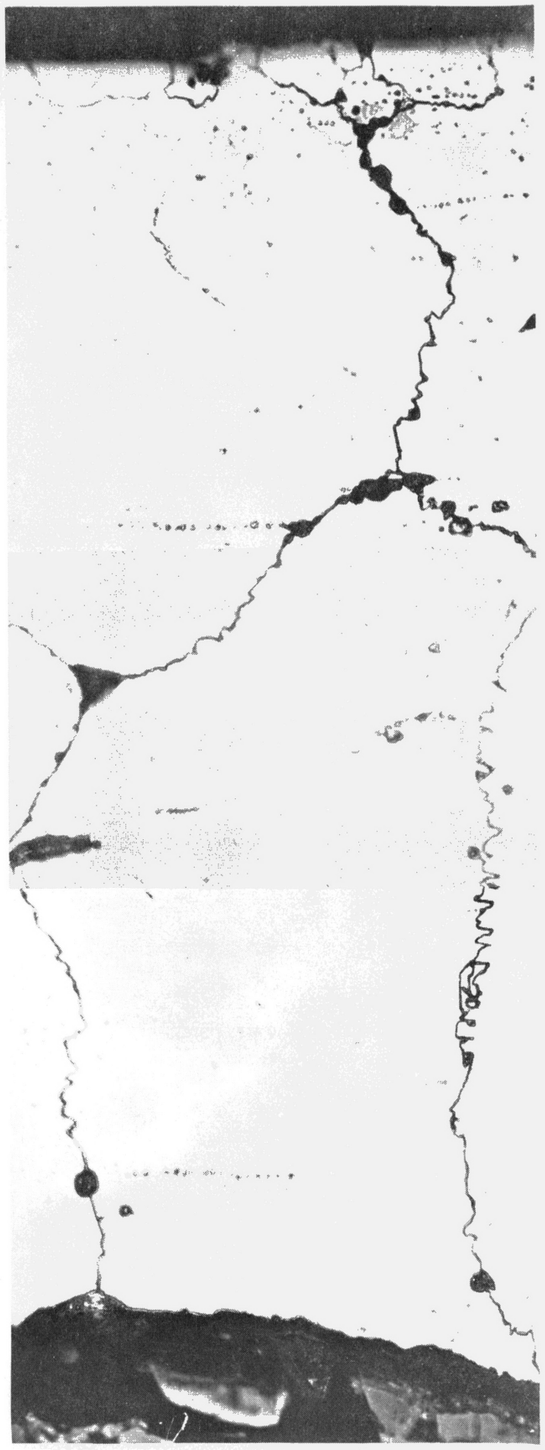

(C)

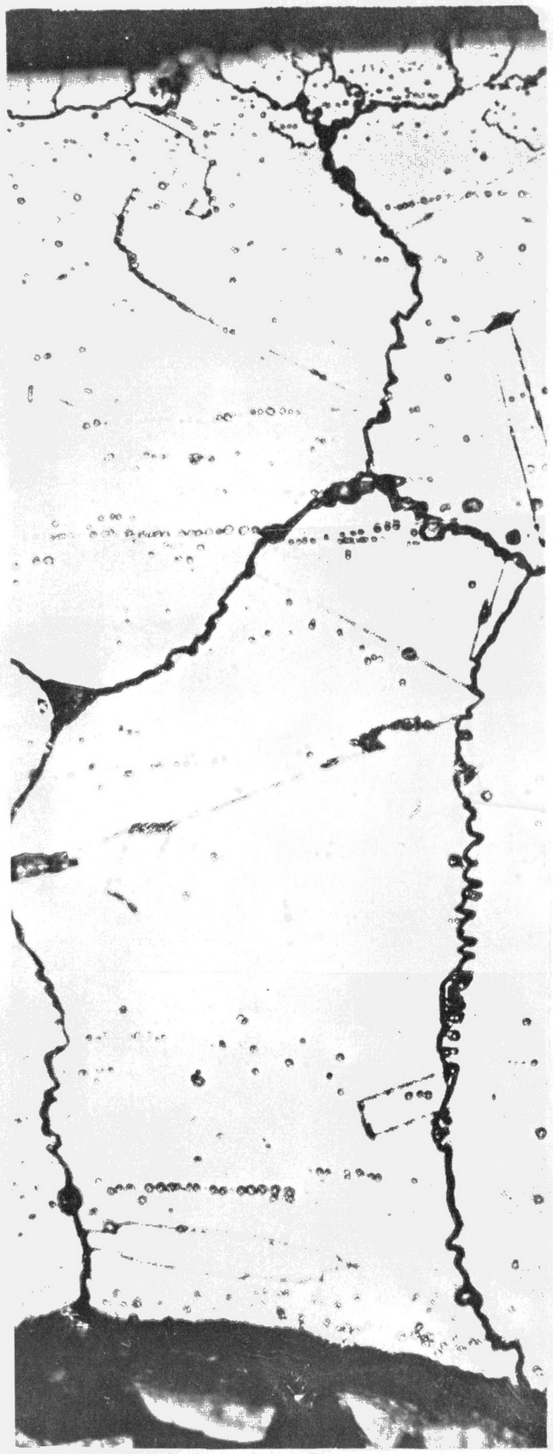

LEGEND

PHOTO (a)

MAG.: 500X

ETCHANT: VILELLA'S

PURPOSE: ATTACKS AUSTENITE; OTHER PHASES IN RELIEF.

PHOTO (b)

MAG.: 500X

ETCHANT: MURAKIMI'S

PURPOSE: ATTACKS CARBIDES

PHOTO (c)

MAG.: 500X

ETCHANT: 10% CHROMIC ACID; ELECTROLYTIC

PURPOSE: ATTACKS SIGMA PHASE AND CARBIDES

1136–18

FIGURE 17 IDENTIFICATION OF PHASES IN FAILURE AREA OF FUEL ROD.

(A)

(B)

(C)

LEGEND

PHOTO (a)

MAG.: 500X

ETCHANT: VILELLA'S

PURPOSE: ATTACKS AUSTENITE; OTHER PHASE IN RELIEF

PHOTO (b)

MAG.: 500X

ETCHANT: MURAKIMI'S

PURPOSE: ATTACKS CARBIDES

PHOTO (c)

MAG.: 500X

ETCHANT: 10% CHROMIC ACID; ELECTROLYTIC

PURPOSE: ATTACKS SIGMA PHASE AND CARBIDES

1136–12

FIGURE 18 IDENTIFICATION OF PHASES IN NON-FAILURE AREA OF FUEL ROD

The identification of the precipitate was determined by etching for carbides, ferrite and sigma phase. Photographs of the clad in failure and nonfailure areas which were obtained during the investigation, are shown in Figures 17 and 18 respectively. The investigation indicated that carbides, sigma phase, and ferrite are present in the grains and at the grain boundaries of both samples of clad. The presence of a carbide precipitate is indicated in photograph b while the presence of sigma phase is proven by comparing photographs c (carbides and sigma phase etched) and b (carbides etched). The presence of ferrite is proven by comparing photograph a (austenite etched; ferrite, sigma phase, and carbides in relief) with photograph c.

The depletion of the carbon near the grain boundaries, by the carbide precipitate, is quite evident in Figure 18. A single layer of fine grains was probably produced by recrystallization and grain growth following the cold swaging and second pressing operation.

The diamond pyramid hardness of the failed fuel rods in a nonfracture area varied from 215 to 254 with an average of 241. The hardness in the vicinity of a fracture varied from 183 to 254 with an average of 225. These hardnesses can be compared with those of the nonirradiated clad 196 for low carbon area to 320 for a high carbon area as reported in the Evaluation of Nonirradiated Materials and Fuel Rods section of this report. These results indicate that irradiation (3×10^{19} nvt) may have produced a slight amount of embrittlement, but not enough to cause the fuel rod failures.

The metallographic examination indicated that the clad material contained large amounts of carbides, ferrite, and sigma phase. These precipitates, particularly those located at the grain boundaries, produced a structure which is quite susceptible to intergranular corrosion and cracking. The fuel rods, according to the metallurgical examination, failed by intergranular corrosion.

Evaluation of Nonirradiated Materials and Fuel Rods

In support of the post-irradiation examination on the failed hot gas isostatic pressed fuel rods, Battelle initiated a study of unirradiated materials which had been fabricated at the same time as the irradiated rods. These materials were fabricated in an identical manner and were, therefore, retained for possible comparison tests. Additional Type 304L stainless steel tubing from the original stock was supplied to BMI by GE-APED to provide further comparison of the unirradiated materials. The tests employed in this study were designed to determine the various physical, mechanical, and corrosion properties of both the cladding and isostatic pressed fuel assemblies. Because of the limited number of isostatic pressed rod segments available it was necessary to conduct successive tests on the specimens to obtain the desired data.

Properties of Type 304L Stainless Steel Tubing: Samples of the stainless steel tubing used in the initial fabrication were subjected to metallographic examination and hardness determination. These results representing an as-received condition were then compared with those representing tubing material exposed to an isostatic pressing cycle of one hour at 2100 F and 10, 000 psi. In this case,

the tubing did not contain UO_2 and any effects noted could, therefore, be attributed to the heat treatment or autoclave atmosphere. Representative structures of the material in both conditions are shown in Figure 19. A marked increase in grain size is evident due to the pressing cycle, an effect noted in previous fabrication of the isostatic pressed fuel rods. Grain boundary precipitates are not apparent suggesting that the pressing treatment would not cause embrittlement of the cladding. The Diamond Pyramid Hardness (DPH) of the as-received material was 301 (29Rc), which is characteristic of a 5 to 10 per cent cold worked steel. The DPH hardness of the fabricated cladding was 196 (90 Rb) which is representative of annealed stainless steel.

The as-received tubing was analyzed chemically and spectrographically revealing a normal analysis except for a slightly high carbon level. The carbon level was further checked on several other samples and also on tubing which was exposed to a pressing cycle without UO_2. The results of the analyses listed in Table III indicate that the starting material did not cause the effects noted in the irradiated rods.

The remaining portions of this tubing which were isostatic pressed were exposed to a Huey Test to determine uniformity of the material. Because of the slow cool from the pressing temperature carbon variations, if present, would result in grain boundary precipitation at such areas. The test, which consists of exposure to boiling 65 per cent HNO_3, would then result in increased attack of the grain boundaries of these areas. Examination of the tubing after two 48 hour exposures in this environment revealed a uniform surface with only slight grain outlining. The extremely small weight changes indicated a uniformly low carbon level in the material.

Upon completion of the Huey Test the tubing sections were slit, flattened, and machined into flat tensile specimens. Similar tensile specimens were made from the as-received tubing for comparison. The data which are listed in Table IV show a decrease in tensile and yield strengths and an increase in elongation due to the pressing treatment. These values are, however, characteristic of annealed type 304 stainless steel and represent an annealing of the apparent cold worked structure in the as-received material.

Properties of Fuel Rod Segments: The isostatic pressed stainless steel clad UO_2 rod segments remaining from the initial fabrication of the VBWR test rods were used to conduct a series of tests intended to establish possible causes for the fuel rod failures. Rod segments measuring 12 and 24 inches long with integral end plugs were available and permitted thermal cycling and corrosion tests of complete segments. Additional tests performed on these and other rods included bend tests, clad tensile tests, metallographic examination, chemical analysis and tap water corrosion of the cladding material.

AS RECEIVED

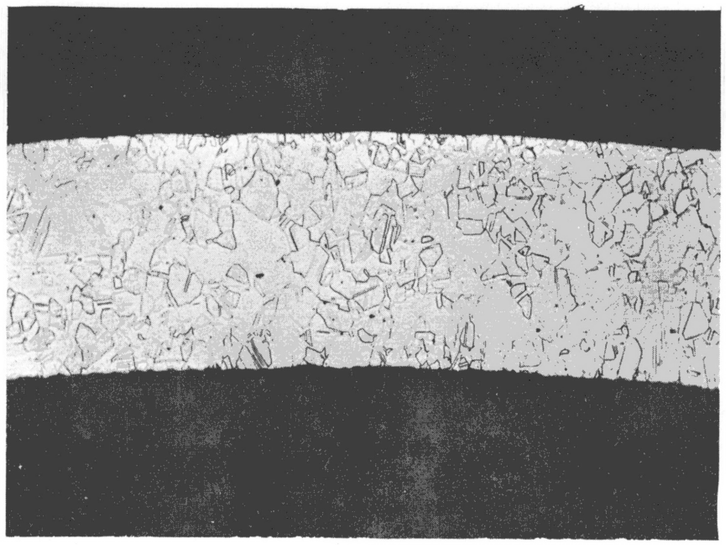

MAGNIFICATION 100X

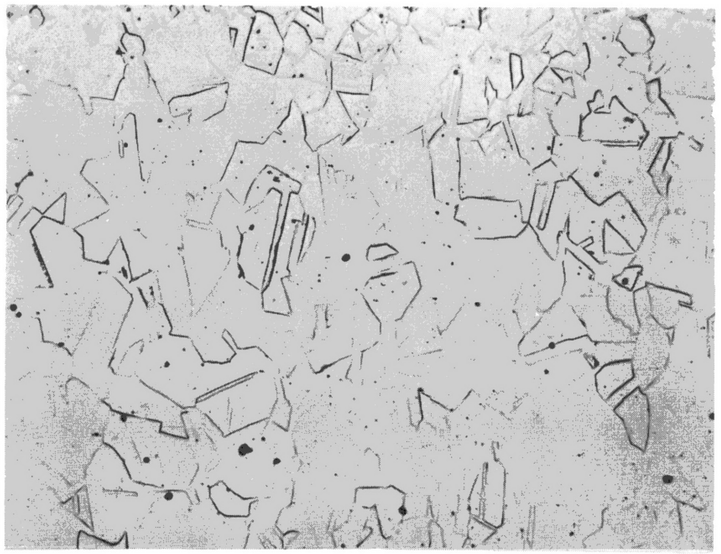

MAGNIFICATION 250X

HOT GAS ISOSTATIC PRESSED

MAGNIFICATION 100X

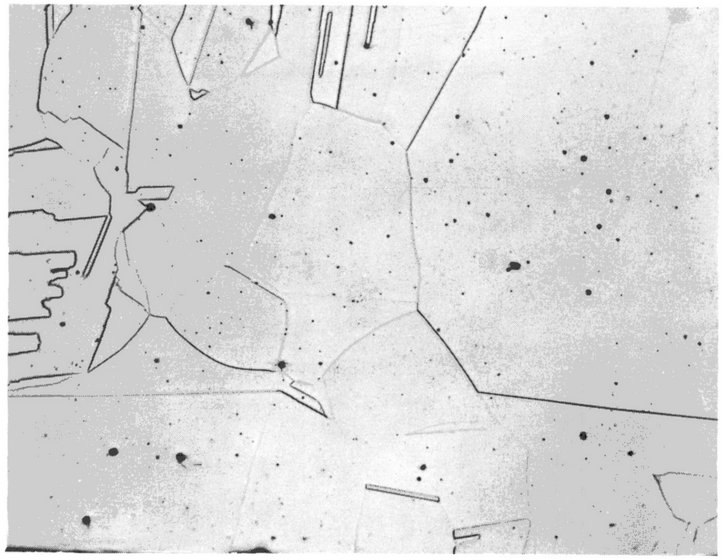

MAGNIFICATION 250X

1136–13

FIGURE 19 COMPARISON OF THE CLAD STRUCTURES IN THE AS-RECEIVED AND HOT GAS ISOSTATIC PRESSED CONDITIONS

TABLE III

ANALYSIS OF TYPE 304L STAINLESS STEEL TUBING

Material Condition	Analysis, w/o													
	C	Mn	Si	Cu	Ni	Cr	V	Mo	Co	Nb	Ti	W	B	Al
As received	0.04	1-1.5	0.2-0.5	0.05-0.1	8-10	17-20	0.02-0.04	0.1-0.2	0.05-0.1	<0.01	<0.002	0.1-0.2	Nd	Nd
As received*	0.029	0.65	0.38	< 0.1	8.1	17.8	--	< 0.1	--	--	--	--	--	--
As received	0.047	--	--	--	--	--	--	--	--	--	--	--	--	--
Bonding Cycled	0.034	--	--	--	--	--	--	--	--	--	--	--	--	--

*GE-APED

TABLE IV

TENSILE PROPERTIES OF THE AS-RECEIVED AND ISOSTATIC PRESSED CLAD MATERIALS

Specimen Condition	0.2% Yield Strength psi	Ultimate Tensile Strength psi	Elongation Percent	Diamond Pyramid Hardness
As-received, BMI test	91,300	112,000	21.8	
	89,200	113,000	26.0	301
	93,500	113,000	25.1	
GE-APED test*	85,200	108,600	33.0	260
Isostatic pressed	48,000	82,500	37.8	
	38,500	76,700	29.3	196
	39,500	82,500	38.7	
	40,800	82,900	36.1	

*Tensile properties obtained using a section of the tubing rather than a flattened section.

A 12 inch isostatic pressed rod segment (IR-12-7) containing pressed end plugs and a sealed evacuation stem was cycled 20 times between room temperature and 1900 F without any significant changes in dimensions or clad surface appearance. This test was conducted in a helium atmosphere such that cold helium provided a rapid cool of the clad surface during the cooling cycle. Heating and cooling times for the clad surface were approximately five minutes as monitored by thermocouples. Although these conditions were not as severe as those expected in-pile, the results suggest that a ratcheting effect did not contribute to the fuel rod failures noted.

A 24 inch long rod segment (IR-24-6) with pressed end plugs was exposed to 550 F water for 500 hours. The surface of the rod after testing appeared normal for stainless steel with a surface coloration varying from a straw color to a very dark tarnish. The weight gain noted was considered high and was reduced to a normal level by baking which would indicate a possible defect in the cladding. Several such defects were located by helium leak testing. On the basis of these results it appears that the gross clad embrittlement and rust colored deposits observed during the RML examination were not caused by corrosion effects in high temperature water. The presence of leaks, however, after testing indicates that some localized attack may have occurred.

Bend tests were performed on the two rods which were thermal cycled and corrosion tested, respectively. The purpose of these tests was to determine if the isostatic pressed composite rod was characteristically brittle. The thermal cycled rod represented an annealed and quenched clad structure whereas the corrosion test rod cladding was essentially in the as-fabricated condition.

Bending in both cases was accomplished by placing the rods on blocks six inches apart in a Carver Hand Press and loading until a 90 degree bend was achieved. The thermal cycled rod was bent 90 degrees at two points, straightened and then bent by hand as shown in Figure 20. Helium leak testing of this rod revealed a slight leak at one of the 90 degree bends. The corrosion tested rod was also found to be quite ductile in two 90 degree bends, however, cracks did appear in the cladding at the point of bending.

Three rod sections were selected for further cladding tensile tests. The cladding on these rods was slit, removed from the UO_2 core, flattened, and machined into flat tensile specimens. Two of the rods, IR-24-5 and IR-12-5 provided little difficulty in clad sampling although one surface retained a considerable UO_2 coating due to the core-clad bonding. On flattening cladding strips from the third rod section (IR-12-8) considerable cracking in isolated areas was noted. Consequently, the cladding strips from this rod were retained for metallographic examination and corrosion tests. The results of tensile tests from this series are listed below where significant increases in tensile and yield strengths and corresponding decreases in elongation values are noted. A comparison of these results with those obtained on tubing material subjected to a bonding cycle suggests contamination due to the contained UO_2 during fabrication.

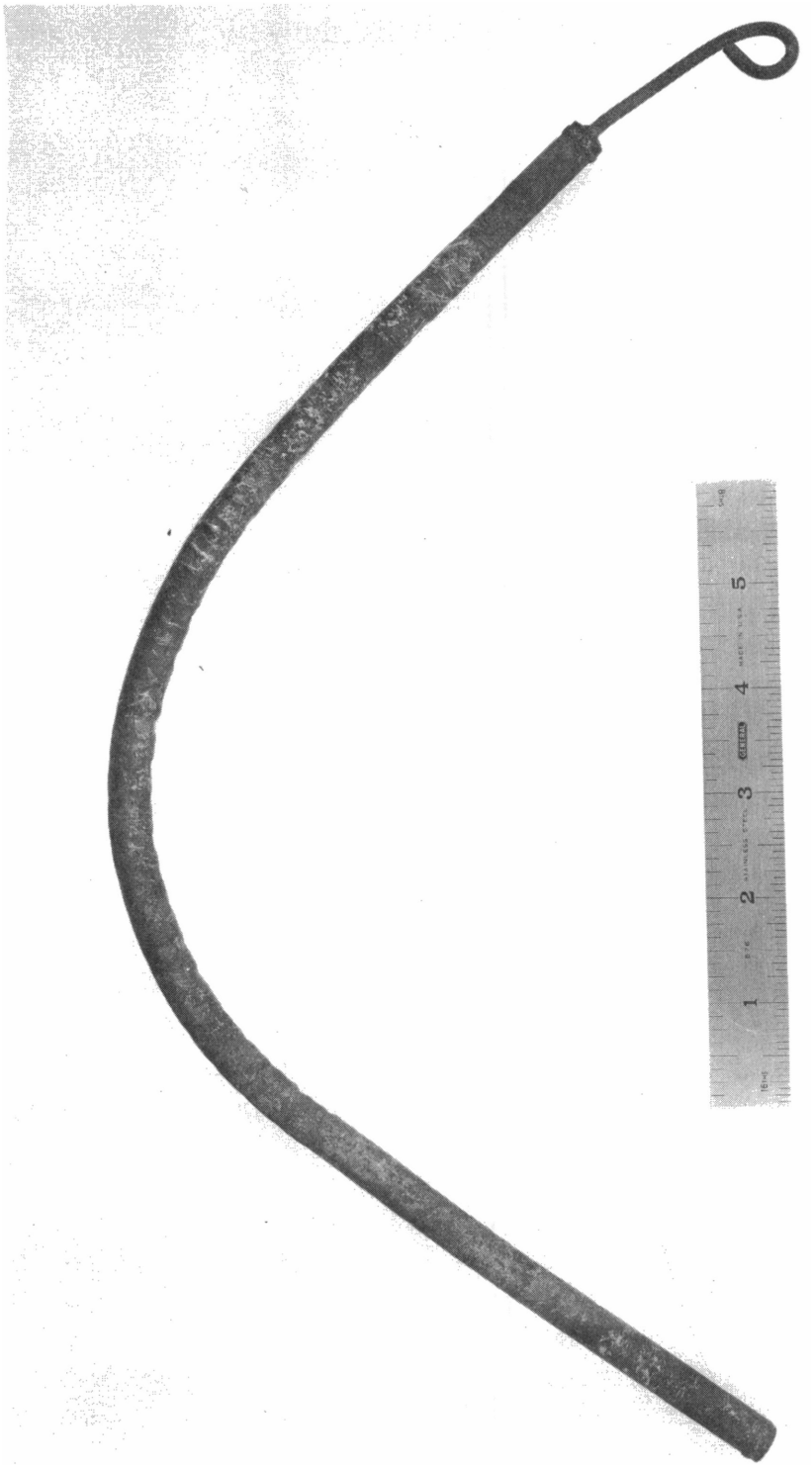

1136–14

FIGURE 20 HOT GAS ISOSTATIC PRESSED STAINLESS STEEL CLAD UO_2 FUEL ROD AFTER THERMAL CYCLING AND BEND TESTING.
ROD WAS BENT 90 DEGREES IN TWO AREAS PRIOR TO BENDING INTO THE ABOVE SHAPE.

Rod Identity	0.2% Yield Strength, psi	Ultimate Tensile Strength, psi	Elongation Per Cent
IR-24-5	---	91,600	25.1
IR-12-5	57,500	90,000	14.1
	54,700	96,500	23.6

Metallographic examination was conducted on cladding samples including the brittle areas from rod IR-21-8. A complete rod (IR-12-6) was ground along its full length, polished and then examined for cladding structure uniformity. All areas of this sample were similar to that noted in the tubing exposed to a pressing cycle as discussed previously. As can be seen from a representative structure shown in Figure 21, large grains with no grain boundary precipitation were evident. In contrast extremely heavy grain boundary precipitation was shown in the microstructure of the brittle clad areas of rod IR-12-8. Such a structure which had an average DPH of 320 (31Rc) is shown in Figure 22. The most likely cause for this extent of grain boundary phase would appear to be excessive carbon resulting in heavy carbide precipitation during cooling in the bonding cycle. A sample of this material was exposed for 72 hours in 550 F water resulting in no apparent corrosion attack. A microstructure of this sample shown in Figure 23 shows separation at the grain boundaries and the apparent removal of several grains from the structure. These events occurred during the removal of the UO_2 core rather than during the corrosion test. The cracking propagated from the inside surface of the clad which was placed in tension by the flattening operation. Areas of the structure near the surface showed no corrosion penetration.

Carbon analyses were run on cladding samples from the various pressed rods available to this study. A number of samples were taken from rod IR-12-8 to check carbon contents at various positions in the rod. In this case the center of the rod represented the highly embrittled area of the cladding. Samples from other bonded rods were taken randomly as no unusual surface effects indicated the need for selective sampling. The results of these analyses which compare to levels of 0.037 to 0.047 w/o carbon for the as-received and isostatic pressed tubing are given in Table V. It is evident that the carbon levels are quite variable with the highest values obtained on samples from the center of rod IR-12-8. End samples from this rod show a lower carbon level which is still much higher than the initial carbon content. These results strongly suggest that residual binder entrapped in the rods during outgassing was the probable cause for the excessive carbon levels. It is interesting to note that rod IR-21-6 which was surveyed extensively for clad structure and found comparable to the initial structure shows only a slight increase in carbon.

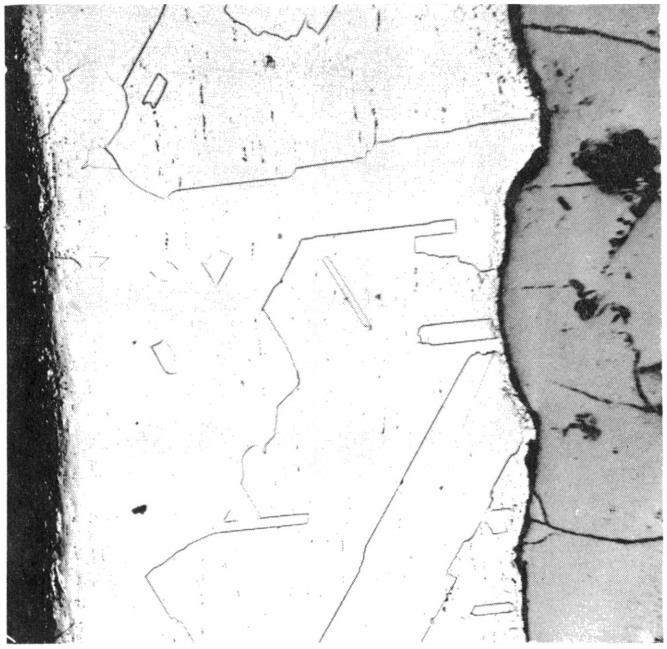

MAGNIFICATION: 100X

KNOOP HARDNESS: 184 (86 Rb)

FIGURE 21 CLADDING STRUCTURE OF HOT GAS ISOSTATIC PRESSED FUEL ROD SEGMENT IR–12–6

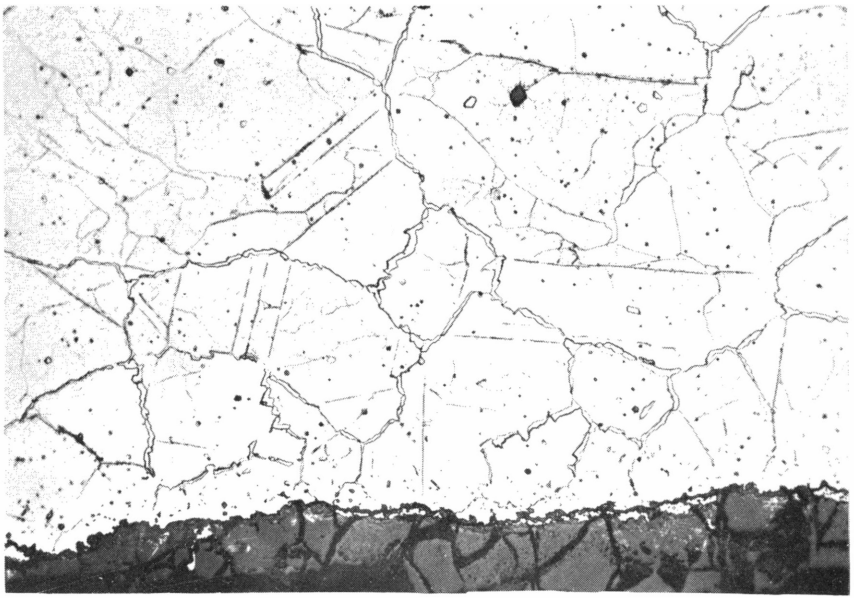

MAGNIFICATION: 250X

1136–15

FIGURE 22 MICROSTRUCTURE OF THE BRITTLE CLAD AREA IN THE HOT GAS ISOSTATIC PRESSED ROD IR–12–8

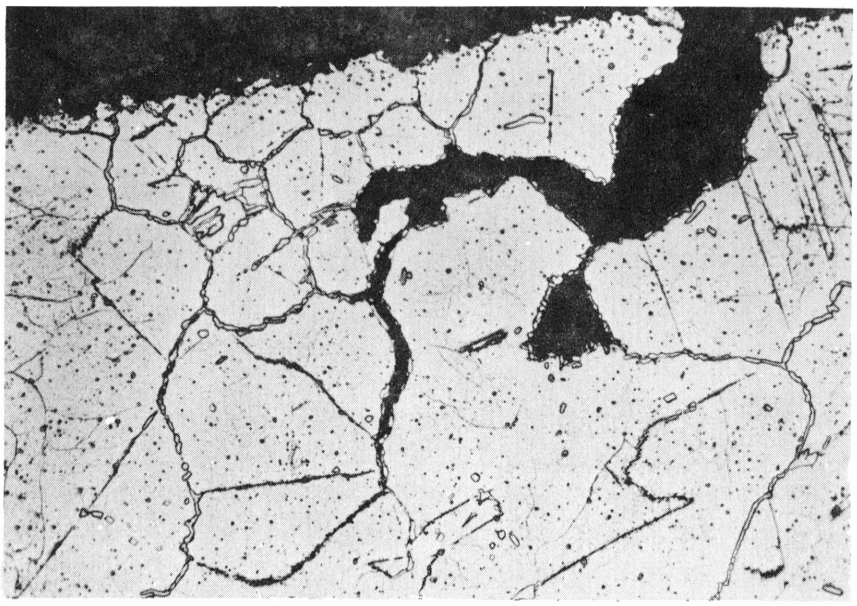

MAGNIFICATION 250X

1136–16

Figure 23. Intergranular Cracking in the Hot Gas Isostatic Pressed Cladding From Rod IR-12-8 After Corrosion Testing for 72 Hours in 550 F Water

TABLE V

CARBON CONTENTS OF CLADDING SAMPLED FROM

HOT GAS ISOSTATIC PRESSED FUEL ROD SEGMENTS

Rod Identity	Sample Location	Carbon, w/o
12-8	Center	0.40
12-8	Center	0.52
12-8	Center	0.50
12-8 (a)	End	0.15
12-8 (a)	End	0.20
12-5 (b)	Random	0.14
12-6 (c)	Random	0.058
24-5	Random	0.4
12-7 (d)	Random	0.19

(a) Approximately 5 inches from center of rod.
(b) Tensile data obtained on this cladding.
(c) Metallographic survey showed uniform structure.
(d) Thermal cycled and bend tested rod.

In view of the high carbon levels noted in the cladding representative samples of UO_2 were also submitted for carbon analyses. Initial carbon levels of the starting oxides were established at 0.013 w/o for the ceramic grade and 0.003 w/o for the fused grade which provided an 0.007 w/o average in the 60-40 mixture used in the fabrication of these rods. A variability in the limited number of samples was also noted in this case as shown in Table VI. The analysis of oxide from the center of rod IR-12-8 is particularly interesting since this high level corresponds to the highest carbon level found in the cladding.

Computations based on the 1 w/o Cerumel C addition to the initial oxide mixture, estimates of the wax content of the binder, and estimates of contained carbon indicate that the carbon levels observed in the cladding and pressed oxide could be related to the binder. Considering that the binder which was used could be approximated by 25 per cent beeswax in water, carbon levels of 0.45 w/o in the UO_2 and 0.35 w/o in the cladding could result. These values are based on uniform distribution of the binder and each case assumes that all of the carbon remains in the respective portion of the rod. In view of possible nonhomogeneities in the material it is particularly noteworthy that the appropriate orders of magnitude are represented by these values.

TABLE VI

CARBON CONTENTS OF HOT GAS ISOSTATIC PRESSED URANIUM DIOXIDE[a]

Rod Identity	Sample Location	Carbon, w/o
IR-12-8	Center	0.079
IR-12-8	End	0.005
IR-12-7	Random	0.003
IR-24-5	Random	0.007

(a) Initial carbon level of oxide mixture was 0.007 w/o

Samples of the high carbon clad and the entire rod IR-24-6, which had previously been corrosion tested in 550 F water and bend tested, were exposed to ordinary tap water to approximate VBWR pool storage conditions. The specimens containing more than 0.3 per cent carbon exhibited the rust colored deposit after very short exposure in tap water. After continued exposure the rust colored samples could be easily broken. Rod IR-24-6 also showed random rust colored spots which included both defect and nondefect areas in the clad.

These results indicate that the rust colored areas contain extremely large amounts of carbon which were susceptible to very rapid intergranular corrosion in room temperature tap water. Consequently, the five month storage of the irradiated rods in the VBWR pool resulted in extensive intergranular corrosion which eventually led to the brittle failure of the fuel rods.